

Mineral surface modification induced by low energy ion irradiation: Implications for solar-wind exposure effects in lunar soil

ZHU Yongchao^{1,2}, FU Xiaohui^{1*}, XU Lin^{1**}, ZHANG Feng¹, ZHENG Yongchun^{1,3}, and ZOU Yongliao¹

¹ Key Laboratory of Lunar and Deep Space Exploration, National Astronomical Observatories, Chinese Academy of Sciences, Beijing 100012, China

² University of Chinese Academy of Sciences, Beijing 100049, China

³ Space Science Institute, Macau University of Science and Technology, Macau, China

* Corresponding author, E-mail: fuxh@bao.ac.cn, ** xul@nao.cas.cn

Received March 2, 2014; accepted June 20, 2014

© Science Press and Institute of Geochemistry, CAS and Springer-Verlag Berlin Heidelberg 2014

Abstract We performed ion irradiation on olivine and ilmenite to simulate solar-wind exposure effects in lunar soil. The surface morphology and microstructure after ion irradiation were characterized by field emission scanning electron microscopy. Sputtering erosion significantly modified the surface of irradiated Luobusha olivine grains. All irradiated grains show smooth surface and round shape. The cleavage fractures on the unirradiated olivine surface were widened and deeply etched after He⁺ irradiation. Both of these are the consequence of ion sputtering erosion. There are no bubbles or voids found in the irradiated olivine grains, because He⁺ dose in this study is lower than saturated fluence. Irradiated Panzihua ilmenite grains are all covered with smooth flakes with the thickness of about 400 nm. The formation of the flakes should be related with helium bubbles and their growth during He⁺ implantation. Some columnar-shaped particles are found at the surface of irradiated Panzihua ilmenite. We speculate that these particles should be sulfide because of significantly high sulfur contents.

Key words space weathering; solar wind; sputter erosion

1 Introduction

Airless bodies of the Solar System, such as the Moon and the Mercury, are continuously exposed to the bombardments of photons, meteorites of different sizes, cosmic rays and solar particles (ions from flares and solar wind, a rarefied plasma made of electrons, protons, heavier ions and magnetic fields streaming radically from the Sun). Space weathering is the physical and chemical alteration of surfaces of airless bodies exposed to the space environment. To investigate energetic ion effects, several experiments have been performed to simulate low-energy ion impact on minerals (Strazzulla et al., 2005; Brunetto and Strazzulla, 2005; Marchi et al., 2005; Loeffler et al., 2009; Fu et al., 2012). Previous investigations have confirmed amorphization and chemical changes in olivine

after low-energy ion irradiation. It is shown that irradiation of a few to tens KeV H⁺ and He⁺ ions can effectively cause amorphization of olivine and enstatite (Demyk et al., 2001; Carrez et al., 2002; Jager et al., 2003). Irradiation of He⁺ or H⁺ ions forms bubbles inside the target material and a high dose irradiation deforms surface structures of the target observed on silicates as orange skins or blisters (Mastsumoto et al., 2013). All the irradiated silicates have shown darkening and reddening of reflectance spectra in the visible and near-infrared (VNIR) range. However, irradiated ilmenite (an opaque Fe-Ti oxide mineral in lunar mare soil) exhibits higher reflectance and stronger absorption features (Fu et al., 2012). This is completely different from lunar soil and analog silicate materials in other experiments, which cannot be explained by the lunar-style space weathering model. But these ex-

periments are far from enough. Firstly, surface modification caused by low energy particles has not been well characterized. Secondly, most of these simulations only focus on mafic minerals, such as olivine and pyroxene while ilmenite has not been investigated.

In the present study, we have performed ion irradiation on olivine and ilmenite to simulate ion implantation on lunar surface. The surface morphology and microstructure after ion irradiation were characterized by field emission scanning electron microscopy (FE-SEM). Secondary electron images with nm-scale resolution will help us find the clue to different spectral modifications between irradiated silicate and ilmenite.

2 Samples and experiments

Natural minerals such as olivine and ilmenite were selected as the samples in the experiments. Olivine is one of the most significant rock-forming minerals on the Moon, Mercury, and asteroids. Ilmenite is composed of titanium and iron oxide, which is the most abundant opaque mineral in lunar rocks. Luobusha olivine ($\sim\text{Fo}_{80}$) is picked from the formation of dunites in the Luobusha ophiolite, southern Tibet. Panzihua ilmenite was sampled from the Panzihua ilmenite deposit in southwestern Sichuan Province of China. The samples were crushed by means of an agate mortar and pestle and sieved (50 mesh) to obtain $<300\ \mu\text{m}$ size-d fraction. The grains were stucked on a silicon wafer ($\Phi 4\ \text{cm}$) using solid epoxy resin as the binder. The ultrasonic cleaning method was employed to clean the mineral grain surface with acetone as a cleaning solvent.

He^+ implantation was performed using an LC-4 high-energy ion implanter at the Institute of Semiconductors, Chinese Academy of Sciences. The experiments were carried out at room temperature, in an ion pumped ultra-high vacuum (UHV) chamber with the residual pressure of 10^{-7} mbar. The energy of ^4He ions is 50 keV. The duration of implantation was 2 hours with the irradiation dose being 5×10^{16} ion/cm². Beam current density was maintained below $45\ \mu\text{A}/\text{cm}^2$ and the ion beam was scanned homogeneously over the target in order to prevent heating during implantation. More details are available from Fu et al. (2012). Both unirradiated and irradiated samples were observed and analyzed using Carl Zeiss SUPRA 55FE-SEM equipped with the Oxford energy dispersive spectrometer (EDS), at the National Astronomical Observatories, China Academy of Sciences. The mineral grains were attached with a double-sided carbon tape. Most of them were coated with carbon or chromium to avoid charge-up effect during the FE-SEM observation. Some were not coated with any electric

conductor, but observed with a low accelerating voltage ($<3\ \text{keV}$) with the SE2 and InLens detectors.

3 Results and discussion

3.1 Sputtering erosion on olivine

Figure 1 compares the SEM images under low magnification ($150\times$) of unirradiated and irradiated Luobusha olivine grains. It was noted that all unirradiated grains display acute angles and sharp edges. However, other irradiated olivine grains show smooth surface and rounded shape. The textures on the mineral surface became unclear and the sharp edges seem cut down. Surface modification of irradiated grains could be attributed to sputtering erosion due to the simulation of solar wind, which had been found in Apollo soils (Pillinger, 1979).

Shown in Fig. 2 is the FE-SEM using secondary electron images of unirradiated and irradiated Luobusha olivine grains. Cleavage is easy to be recognized on the surface of olivine grains. For unirradiated olivine, the perfect cleavage fractures are long and narrow and parallel to each other. Olivine usually shows two groups of cleavages [010] and [100]. After He^+ irradiation, these linear fractures widened and were deeply etched. The deep grooves display a U/V shape cross-section, $2\text{--}3\ \mu\text{m}$ in length and $0.3\text{--}0.6\ \mu\text{m}$ in width. Li et al. (2013) found that He^+ ions injected along [010] would damage the olivine structure more effectively than with other orientations. This is consistent with only one group cleavages on the irradiated olivine surface.

Previous studies noted that olivine samples irradiated with He^+ ions at a high dose showed numerous blister structures on their surfaces with TEM (Demky et al., 2001) and SEM (Matsumoto et al., 2013). That is because implanted helium tends to aggregate into bubbles and the diameter of bubbles increases with ion dose. However, there were no bubbles or voids observed on the irradiated olivine surface in this study. He^+ fluence in this study is 20 times lower than the saturated fluence of $10^{18}/\text{cm}^2$ (Futagami et al., 1993), which should explain why there are no bubbles for irradiated Luobusha olivine.

3.2 Surface morphological modification on ilmenite

For ilmenite, morphological changes due to He^+ irradiation are distinguished from Luobusha olivine. Irradiated Panzihua ilmenite did not show sputtering erosion on the surface but were all covered with smooth flakes with the thickness of about 400 nm (Fig. 3). The flakes' thickness is consistent with the most damaged depth of 390 nm of Panzihua ilmenite

calculated by the SRIM program (at <http://www.SRIM.org/>, Ziegler et al., 1985).

Futagami et al. (1993) interpreted that the surface layer was flaked off due to gas pressure in large bubbles. Helium bubbles (voids) were also found on grain edges of some irradiated ilmenite. Ion implantation produced sponge-like microstructure for the parts with

high-density bubbles. However, no bubbles or voids were noted on the smooth flakes of irradiated ilmenite but just the rings, although the formation of helium bubbles in metal after He⁺ irradiation has already been reported in numerous studies (Trinkaus, 1983). The round orelliptical rings should be the residual mark of helium bubbles that already released all gases.

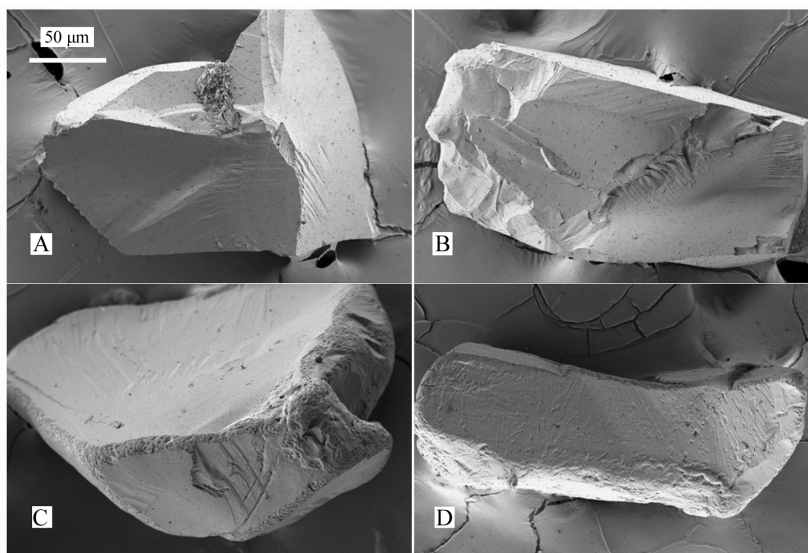


Fig. 1. Comparisons of unirradiated and irradiated Luobusha olivine grains. A and B indicate the unirradiated olivine grains while C and D stand for the irradiated olivine by 50 keV He⁺.

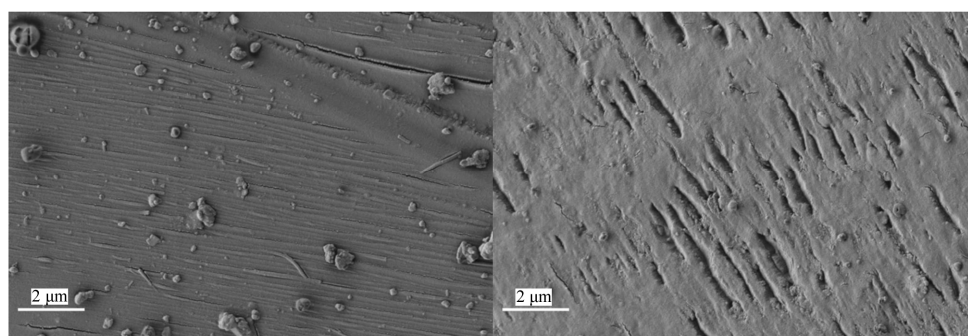


Fig. 2. SEM images of unirradiated (left) and irradiated (right) Luobusha olivine surface.

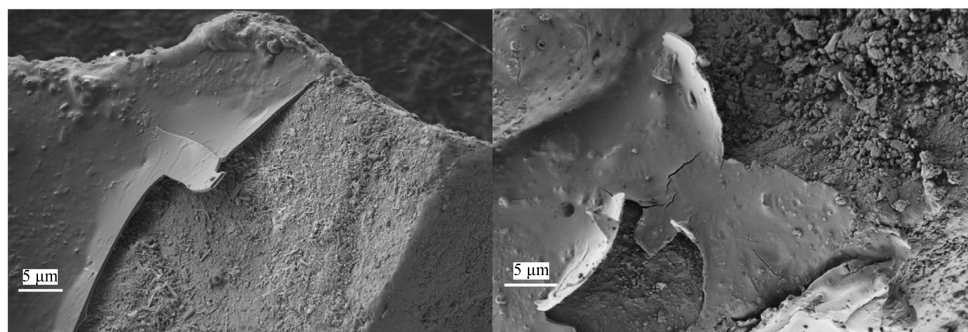


Fig. 3. SEM images of irradiated Panzhuhua ilmenite grains.

Except these, plastic deformations of the flakes were also recognized for some grains (Fig. 4). Ion implantation could cause rise in surface temperature of the target. However, it is still impossible to cause any melting of ilmenite. Although the formation mechanism of the flakes has not been identified, we could rule out the possibility that they are just produced by irradiation damage. Because irradiation damage accumulation could only lead to surface amorphization of olivine instead of plastic deformation.

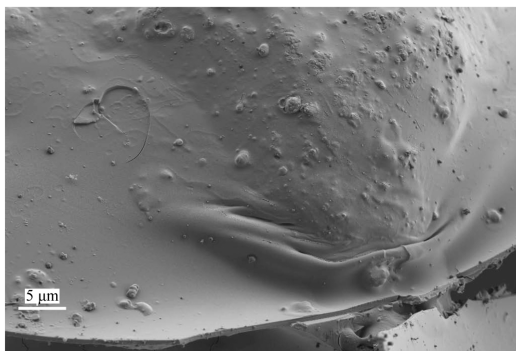


Fig. 4. Plastic deformation of an irradiated Panzihua ilmenite grain. On the flake surface are the blisters due to helium bubbles or voids produced during ion implantation.

Keller and McKay (1997) described four distinct types of rims found on lunar soil grains: amorphous, inclusion-rich, multiple, and vesicular. In this study, the flakes covering irradiated ilmenite look similar with the thin amorphous rims that surrounded micrometer-sized grains in lunar soil. Most amorphous rims are about 50 nm in thickness. For lunar ilmenite, its thickness is about 120 nm (Bernatowicz et al., 1994), which is nearly a quarter of the flake thickness in this study. It seems reasonable to consider that He^+ energy we chose in the experiments is 50 keV and solar wind ion is just 1 keV/amu. Unlike amorphous rims on lunar soil grains, the flakes were detached from the host. This may be related to temperature variation during irradiation and after that. After irradiation, long-term exposure at room temperature could be taken as an annealing process, which resulted in the flakes detaching from the host.

To verify their origin, the composition of flakes was investigated. We performed EDS analyses of the flakes (4 analyses) and host mineral (4 analyses). The analyzed points and chemical compositions are shown in Fig. 5. The results revealed that the Mg peak areas of the flakes seem to be greater than those of the host mineral ilmenite. For refractory elements (Fe and Ti), the peak areas of the flakes and host share the same area. If we take the element peak areas equal as abun-

dance, the result will agree well with Apollo 71501 ilmenite (Bernatowicz, 1994). However, we cannot draw such a conclusion that the flakes are enriched in Mg, just on the basis of the EDS spectra. Differences in Mg abundance between the flakes and the host mineral are negligible, considering the qualitative results of EDS analysis. It is suggested that the flakes surrounding the irradiated ilmenite grains share the same chemical composition with the host mineral. The formation of the flakes should be related with helium bubbles. During He^+ implantation, massive precipitation of helium would lead to sample surface blistering and finally promote flake formation. This is different from the redeposition mechanism of lunar amorphous rims' materials (Keller and McKay, 1997). No flakes on lunar soil grains may be due to the fact that experimental He^+ flux is about 50000 times larger than solar wind flux on the Moon. For the present experiments, high-dose irradiation in 2 hours would lead to the formation of helium bubbles and their rapid growth. Both of them would improve the flake formation on irradiated ilmenite. For Luobusha olivine, sputtering erosion dominates the surface modification during ion implantation. Therefore, no flakes were observed on the irradiated olivine grains.

3.3 Identifying unknown columnar-shaped particles

In addition, some mineral-like particles were found on the surface of irradiated Panzihua ilmenite (Fig. 6). The columnar-shaped particles are generally 1–1.5 μm in length and 0.3–0.5 μm in width. Most of these particles spread over the special area of irradiated ilmenite where the flakes are striped off and the subsurface is exposed. They always mix with small-size ilmenite granules that are usually adhered to the host mineral. It is also noticed that a few of the particles are growing inside the flakes. The direction of long axis distribution possesses no regularity. The particles look like mineral monocrystals. We cannot determine whether they are minerals or just show mineral shape, just with SEM images.

The chemical compositions of these particles were analyzed with EDS (Fig. 7). Ilmenite is composed of Ti, Cr, Fe, and Mg, which is very close to the host in Fig. 5. However, the unknown particles show distinct element composition. Except Ti, Cr, and Fe, they show strong peaks of S and other elements such as Cu, Ca, and Si.

The contamination effect has been considered in this study. Irradiated ilmenite shares the same preparation and storage processes as unirradiated ilmenite, except for He implantation. We observed all the unirradiated ilmenite grains using SEM with high magni-

fications, but no columnar-shaped particles are found. It should be noted that some of the columnar-shaped particles are growing inside the flakes. It seems that they are resultant from the direct precipitation from the flakes. Therefore, the contamination in this experiment could be excluded.

Panzhuhua ilmenite we used in the present study is commonly associated with other sulfides, mostly pyrrhotite and hengleinite (Guo et al., 2011). Sulfur and other elements may be derived from these metallic sulfides. Based on these results, we could not identify which minerals they would be. But we can only

speculate that these columnar-shaped particles should be sulfides because of their significantly high sulfur contents.

Fu et al. (2012) measured the VIS-NIR spectra of original and He⁺ irradiated Panzihua ilmenite. It was noted that irradiated ilmenite displays a new band near 0.87 μm. This corresponds to the characteristic absorption feature of hematite (α-Fe₂O₃), which is due to Laporte-forbidden transitions (Clark, 1999 and references therein). Both of these results may imply that He⁺ irradiation may induce phase transition in Panzihua ilmenite.

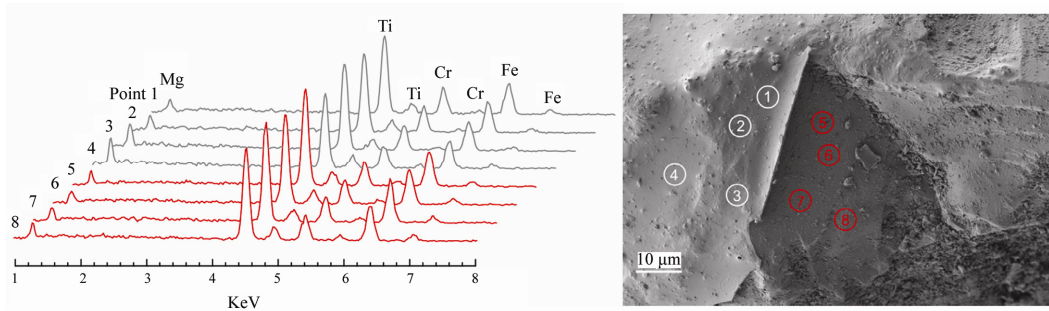


Fig. 5. EDS spectra of the flakes and host ilmenite. The circles and numbers on the right show the analysis points. Points 1–4 are located at the flakes and points 5–8 lie on the host mineral. The ilmenite grain was coated with Cr. Therefore, Cr abundance determined here is not the true value for the sample.

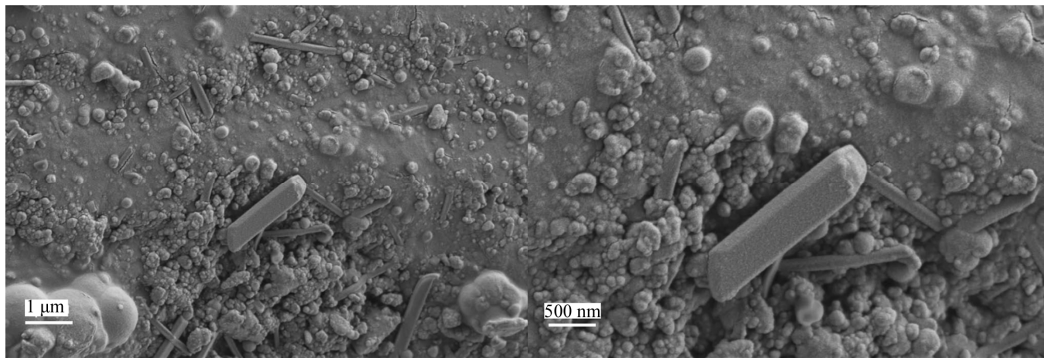


Fig. 6. Unknown columnar-shaped particles on the surface of irradiated Panzihua ilmenite.

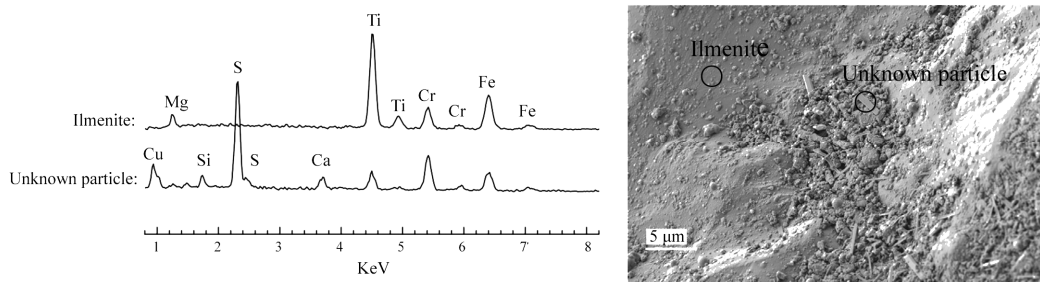


Fig. 7. EDS spectra of the unknown columnar-shaped particles. As talked above, the ilmenite grain was coated with Cr. Therefore, Cr abundance determined here is not the true value for the sample.

4 Conclusions

We performed ion irradiation on olivine and ilmenite to simulate solar-wind exposure effects in lunar soil. Unirradiated and irradiated samples were characterized with FE-SEM/EDS. Several conclusions can be drawn from our new simulation experiments:

(1) Sputtering erosion significantly modifies the surface of irradiated Luobusha olivine grains. All unirradiated grains display acute angles and sharp edges. Irradiated olivine grains show smooth surface and rounded shape, and the cleavage fractures on the olivine surface become widened and are deeply etched. Both of these are the consequence of low-energy ion sputtering.

(2) There are no bubbles or voids observed on the irradiated olivine like the results from previous experiments, because He^+ dose in this study is lower than saturated fluence.

(3) Irradiated Panzhihua ilmenite is all covered with smooth flakes with the thickness of about 400 nm. The formation of the flakes should be related with helium bubbles and their growth during He^+ implantation. Some mineral-like particles are found on the surface of irradiated Panzhihua ilmenite.

Acknowledgements This research project was financially supported by the National Natural Science Foundation of China (Nos. 41303051 and 41073053).

References

- Bernatowicz T.J., Nichols R.H., and Hohenberg C.M. (1994) *Origin of Amorphous Rims on Lunar Soil Grains* [C]. pp.105. Proc. Lunar Sci. Conf. 25th.
- Brunetto R. and Strazzulla G. (2005) Elastic collisions in ion irradiation experiments: A mechanism for space weathering of silicates [J]. *Icarus*. **179**, 265–273.
- Carrez P., Demyk K., Cordier P., Gengembre L., Grimblot J., D'Hendecourt L., Jones A.P., and Leroux H. (2002) Low-temperature crystallization of MgSiO_3 glasses under electron irradiation: Possible implications for silicate dust evolution in circumstellar environments [J]. *Meteoritics and Planetary Science*. **37**, 1615–1622.
- Clark R. (1999) *Manual of Remote Sensing, Remote Sensing for the Earth Sciences* [M]. pp.3–58. John Wiley and Sons Inc., New York.
- Demyk K., Carrez Ph., Leroux H., Cordier P., Jones A.P., Borg J., Quirico E., Raynal P.I., and d'Hendecourt L. (2001) Structural and chemical alteration of crystalline olivine under low energy He^+ irradiation [J]. *Astronomy & Astrophysics*. **368**, 38–41.
- Fu Xiaohui, Zuo Yongliao, Zheng Yongchun et al. (2012) Effects of space weathering on diagnostic spectral features: Results from He^+ irradiation experiments [J]. *Icarus*. **219**, 630–640.
- Futagami T., Ozima M., Nagal S., and Aoki Y. (1993) Experiments on thermal release of implanted noble gases from minerals and their implications for noble gases in lunar soil grains [J]. *Geochimica et Cosmochimica Acta*. **57**, 3177–3194.
- Guo Yufeng, You Gao, Jiang Tao et al. (2010) Solid-state reduction behavior of Panzhihua ilmenite [J]. *Journal of Central South University (Science and Technology)*. **41**, 1639–1644.
- Jager C., Fabian D., Schrempel F., Dorschner J., Henning T., and Wesch W. (2003) Structural processing of enstatite by ion bombardment [J]. *Astronomy & Astrophysics*. **401**, 57–65.
- Keller L.P. and McKay D.S. (1997) The nature and origin of rims on lunar soil grains [J]. *Geochimica et Cosmochimica Acta*. **61**, 2331–2341.
- Li Yang, Li Xiongyao, Wang Shijie et al. (2013) Crystal orientation results in different amorphization of olivine during solar wind implantation [J]. *Journal of Geophysical Research—Planets*. **118**, 1974–1982.
- Loeffler M.J., Dukes C.A., and Baragiola R.A. (2009) Irradiation of olivine by 4 keV He^+ : Simulation of space weathering by the solar wind [J]. *Journal of Geophysical Research*. **114**.
- Marchi S., Brunetto R., Magrin S., Lazzarin M., and Gandolfi D. (2005) Space weathering of near-Earth and main belt silicate-rich asteroids: Observations and ion irradiation experiments [J]. *Astronomy & Astrophysics*. **443**, 769–775.
- Matsumoto T.M., Tsuchiyama A.T., Takigawa A.T., Yasuda K.Y., Nakata Y.N., Matsuno J.M., Nagano T.N., Shimada A.S., Nakano T.N., and Uesugi K.U. (2013) *Surface Nano-Morphologies of Itokawaregolith Particles Formed by Space Weathering Processes: Comparison with Ion Irradiation Experiments* [C]. pp.1441. Proceedings of Lunar Science Conference 44th.
- Pillinger C.T. (1979) Solar-wind exposure effects in the lunar soil [J]. *Reports on Progress in Physics*. **42**, 897–932.
- Strazzulla G., Dotto E., Binzel R., Brunetto R., Barucci M.A., Blanco A., and Orovino V. (2005) Spectral alteration of the meteorite Epinal (H5) induced by heavy ion irradiation: A simulation of space weathering effects on near-Earth asteroids [J]. *Icarus*. **174**, 31–35.
- Trinkaas H. (1983) Energetics and formation kinetics of helium bubbles in metals [J]. *Radiation Effects*. **78**, 189–211.
- Ziegler J., Biersack J., and Littmark U. (1985) *The Stopping Power and Range of Ions in Solids* [M]. pp.1–40. Pergamon, New York.